Sensors and Materials, Vol. 38, No. 1 (2026) 109–118
MYU Tokyo

S & M 4287

Correlation between Depth-dependent Orientation Structure and Thermal Conductivity of Mesogenic Epoxy Resins

Naoto Kudo,[1] Yoshitaka Takezawa,[2] Tsuyoshi Nishi,[1*] and Hiromichi Ohta[1]

[1]Graduate School of Science and Engineering, Institute of Quantum Beam Science, Ibaraki University, 4-12-1 Nakanarusawa, Hitachi, Ibaraki 316-8511, Japan
[2]Institute for Advanced Integrated Technology, Resonac Corporation, 48 Wadai, Tsukuba, Ibaraki 300-4247, Japan

(Received October 15, 2025; accepted December 2, 2025)

Keywords: thermal conductivity, thermal effusivity, mesogenic epoxy resin, thin film, thermal microscope

The thermal conductivities of mesogenic epoxy (ME) resin films were evaluated by thermal microscopy (TM) based on periodic heating thermoreflectance. A three-layer model, consisting of a glass layer to ensure surface planarity, a Mo layer to generate thermal reflectance signals, and a resin layer as the target for thermal measurement, was used in the analysis. The results revealed that the effective thermal conductivity increased upon decreasing the modulation frequency, reflecting the contributions from film regions at different depths. This behavior indicated a correlation between molecular orientation and thermal transport, which was consistent with the results of the previous reports on ME ordering. This method was also found to be suitable for materials such as polymers, adhesives, and soft substrates, on which direct Mo deposition was not appropriate because of possible thermal damage, or for those facing difficulties in achieving mirror-like surfaces required for TM.

1. Introduction

In recent years, miniaturization and increase in the power density of electronic and power devices have led to a continuous increase in the amount of heat generated within electronic packages, creating a strong demand for improved thermal management inside these devices. Among these limiting factors, polymeric insulating materials, which serve as electrical insulators, generally exhibit low thermal conductivities and have long been recognized as major bottlenecks to efficient heat dissipation.

Mesogenic epoxy (ME) resins are thermosetting epoxy resins modified with mesogenic groups that induce liquid-crystalline behavior, allowing the formation of highly ordered structures during curing. Such ordered structures inhibit phonon scattering, which governs the heat conduction in insulating polymers, resulting in these ME resins exhibiting significantly higher thermal conductivities than conventional epoxy resins.[1–9] Moreover, the molecular orientation of an ME resin exhibits a characteristic dependence on the wettability of the substrate on which it is coated.[10] On hydrophilic substrates, molecules align perpendicular to the surface,

*Corresponding author: e-mail: tsuyoshi.nishi.75@vc.ibaraki.ac.jp
https://doi.org/10.18494/SAM5978

ISSN 0914-4935
https://myukk.org/

whereas on hydrophobic substrates, they align in a parallel direction, resulting in enhanced thermal transport along the respective alignment directions.[11,12] In addition, when molecules align perpendicular to the substrate, the interfacial thermal resistance is lower.[11] In ME thin films on hydrophilic substrates, the molecular orientation varies with the film thickness—molecules are oriented vertically near the substrate interface, randomly toward the middle of the film, and horizontally near the air interface.[13] These different molecular alignments suggest that the thermophysical properties of ME films may be nonuniform at nano- to microscales. A quantitative evaluation of this phenomenon can help advance high-precision thermal designs at these scales.

In this study, we apply a new configuration of the periodic heating thermoreflectance method, in which a laser is irradiated through a glass slide, to clarify the correlation between the depth-dependent molecular orientation distribution and thermal conductivity of ME thin films.

2. Experimental Methods

2.1 Samples

ME thin-film samples were prepared as follows. Two soda-lime glass slides (10×10 mm^2, 1 mm thick) were prepared, and a Mo thin film of 100 nm thickness was deposited on the surface of one slide using a high-frequency sputtering system (SVC-700LRF, SANYU). The ME resin[13] was then coated onto the Mo thin film, where the varnish concentration was adjusted on the basis of a previously obtained relationship between concentration and film thickness to obtain approximately 5 μm after curing. The thickness was also measured after curing using a dropping-cylinder-type micrometer with a measurement area of approximately 1 mm diameter, confirming a variation within ±1 μm. The sample was then sandwiched between the two glass slides and cured, resulting in the configuration presented in Fig. 1. Prior to sample preparation, the ME films coated directly on the Mo thin film and glass substrate were structurally characterized using grazing-incidence small-angle X-ray scattering (GI-SAXS; Rigaku SmartLab). A Hi-Pix-3000 two-dimensional (2D) detector was employed in a 2D GI-SAXS optical system under the following conditions: 40 kV, 30 mA, a camera length of 300 mm, and Cu Kα radiation (λ = 0.15418 nm). In this configuration, the ME thin film was irradiated by a 100 μm collimated X-ray beam at a shallow angle of 0.15°. Owing to the long optical path in the oblique incidence geometry, the detected GI-SAXS signal corresponded to scattered components that were transmitted through the entire film thickness, producing an effective thickness-integrated diffraction profile.

2.2 Thermal microscopy (TM)

In this study, the thermal properties of ME films were evaluated by TM, which is based on the periodic heating thermoreflectance method and is capable of noncontact and nondestructive measurements of thermophysical properties at the micrometer scale.[14] A schematic of the measurement system is presented in Fig. 2. A Mo thin film was deposited on the sample surface

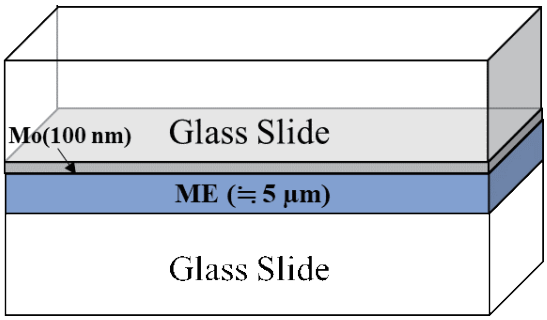

Fig. 1. (Color online) Schematic of a sample.

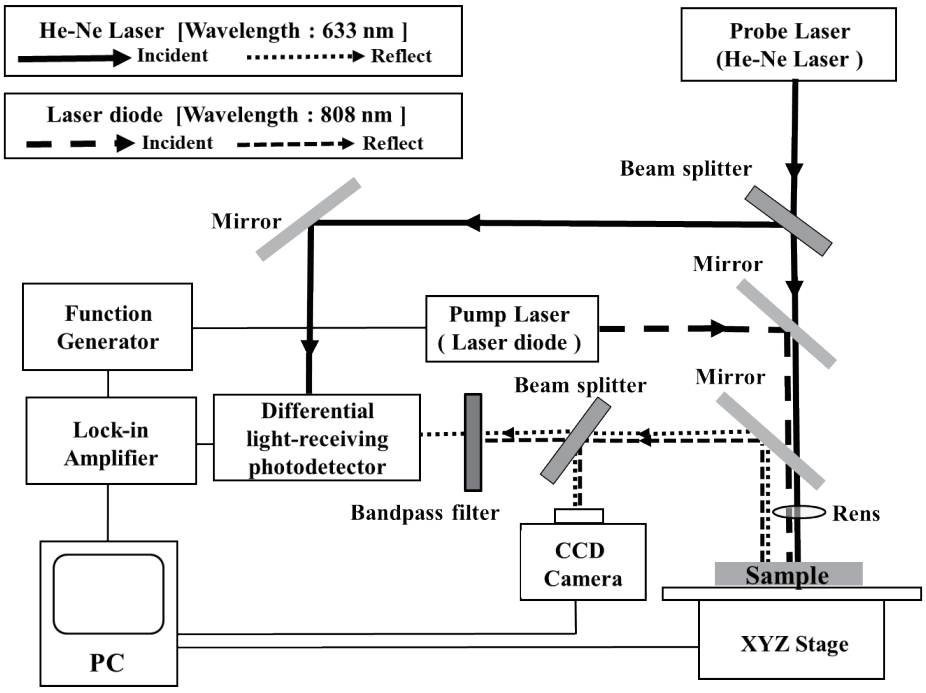

Fig. 2. Schematic of a TM system.

and irradiated using a sinusoidally modulated heating laser to induce periodic heating. The surface of the Mo thin film was irradiated by a probe laser beam, coaxially aligned with the heating beam, which was then reflected from the surface of the Mo thin film. The temperature dependence of metal reflectivity caused its intensity to vary slightly with the surface temperature. The component of this reflected signal at the modulation frequency was detected using a differential photodiode and amplified using a lock-in amplifier, allowing the precise determination of the phase delay of the surface temperature response. Because this phase delay depended on the thermophysical properties of the sample, this analysis facilitated the evaluation of the thermal effusivity of the sample. The spot diameters of the pump and probe lasers were approximately 30 and 10 μm, respectively. Because the pump beam was sufficiently larger than the probe beam, the temperature field within the probed region could be regarded as laterally uniform. Under these conditions, heat conduction in the sample could be reasonably approximated to be one-dimensional (1D) along the thickness direction.

Traditionally, TM analysis, which assumes 1D heat conduction,[14] yields reliable results for low-thermal-conductivity materials, such as glass and ceramics. TM has been applied to a wide variety of samples, including yttrium barium copper oxide superconducting films,[15] Al_2O_3 films,[16] Si–Ge–Au superlattice films,[17] functionally graded materials,[18] and individual particles of lunar regolith simulants.[19,20] Matsui and coworkers introduced an analytical solution that accounted for the heat diffusion in three-layered samples.[21–23] A schematic of a three-layer sample model is presented in Fig. 3. This model treats the air region, metal transducer, and sample as laterally infinite and isotropic layers. The periodically modulated heating laser is modeled as a Gaussian heat flux, and the resulting temperature field is obtained by solving the heat diffusion equation in cylindrical coordinates. Using the Hankel transform, the radial dependence of the temperature field is expressed in the spatial frequency domain, and the amplitudes of the upward and downward thermal waves in each layer are determined from the continuity of the temperature and heat flux at the interfaces. The surface-temperature oscillation detected by the probe beam is then calculated by weighing the solution using the probe-beam profile. This analytical framework accounts for three-dimensional (3D) heat spreading and facilitates the accurate evaluation of the phase delay in multilayer structures. In previous studies, the first layer of the model was treated as a semi-infinite air layer, because measurements were conducted in air. In this study, we replaced the air layer with a semi-infinite glass substrate to account for the thermal properties of glass in the analysis. Because the density and specific heat of the ME sample were known, its volumetric heat capacity was fixed. The thermophysical properties used in this analysis are listed in Table 1. Here, the thermal diffusion length μ for a given modulation frequency f is expressed by Eq. (1) in terms of the heat diffusivity α, thermal conductivity λ, thermal effusivity b, and angular frequency $\omega = 2\pi f$.

$$\mu = \sqrt{\frac{2\alpha}{\omega}} = \sqrt{\frac{\lambda}{\pi\rho C_p f}} = \frac{b}{\rho C_p \sqrt{\pi f}} \tag{1}$$

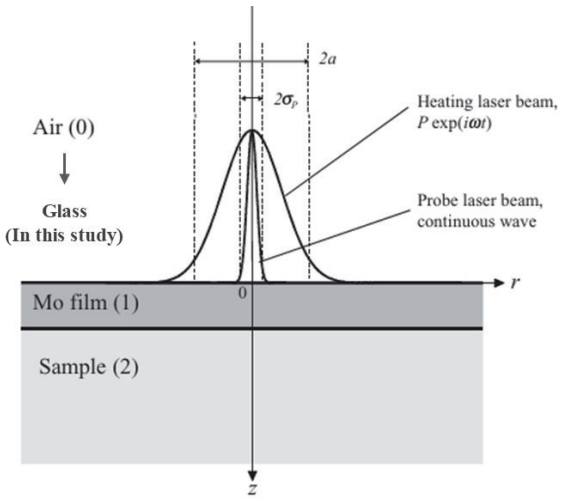

Fig. 3. Schematic of a three-layer sample model.

Table 1
Thermophysical properties of each material used in the analysis.

Material (Layer)	Density (kgm^{-3})	Specific heat capacity ($Jkg^{-1}K^{-1}$)	Thermal conductivity ($m^{-1}K^{-1}$)
Glass Slide (0)	2500	840	0.85
Mo (1)	10200	248	4.34
ME (2)	1230	1250	0.1–10

According to Eq. (1), lowering the modulation frequency increases the thermal diffusion length, thereby increasing the sensitivity to the deeper regions of the sample. Taking advantage of this property, the modulation frequency was varied among 1000, 500, 200, and 100 kHz. For each frequency, theoretical curves of "phase delay vs thermal conductivity" were generated by calculating phase delays while varying the thermal conductivity of the ME from 0.1 to 10.0 $W{\cdot}m^{-1}{\cdot}K^{-1}$ in increments of 0.1. The experimental phase delays were then compared with these curves to extract the thermal conductivity via inverse analysis. By analyzing the results across different frequencies, we investigated the correlation between the depth-dependent molecular orientation and thermal conductivity of the ME thin films. Matsui and coworkers analyzed the 3D heat flow induced by a heating laser with a Gaussian intensity distribution, because their setup involved a narrow heating area.[21–23] In contrast, the system used in this study had a wide heating area, which justified the assumption of 1D heat conduction. This assumption was confirmed by applying Matsui's equation to a more uniform beam profile than the actual profile, which resulted in no significant change in the calculated values.

3. Results and Discussion

3.1 Structural analysis of ME

Figures 4(a) and (b) present the 2D images obtained, while Figs. 4(c) and (d) show the corresponding 2θ and β scans, respectively. In both cases, a sharp peak at approximately $2\theta = 3–4°$ was observed, corresponding to the molecular periodicity of ME (monomer type). In addition, the β scans revealed distinct peaks at an azimuth angle of 90°, indicating that the ME molecules were vertically aligned at both the Mo and glass interfaces. Furthermore, the diffraction intensity suggested that the degree of vertical alignment at the glass interface was higher than that at the Mo interface. From the results of this study and previous studies showing that ME molecules exhibited the highest degree of alignment at contact surfaces, it could be inferred that the fabricated samples adopted the structure illustrated in Fig. 5.

3.2 Thermal conductivity of ME

Figure 6 shows the theoretical curves of the phase delay versus thermal conductivity at each modulation frequency, along with the experimentally obtained phase delays. The error bars along the horizontal and vertical axes represent the variations in the measured phase delays and the thermal conductivity estimated from these phase delays, respectively. Because the thermal

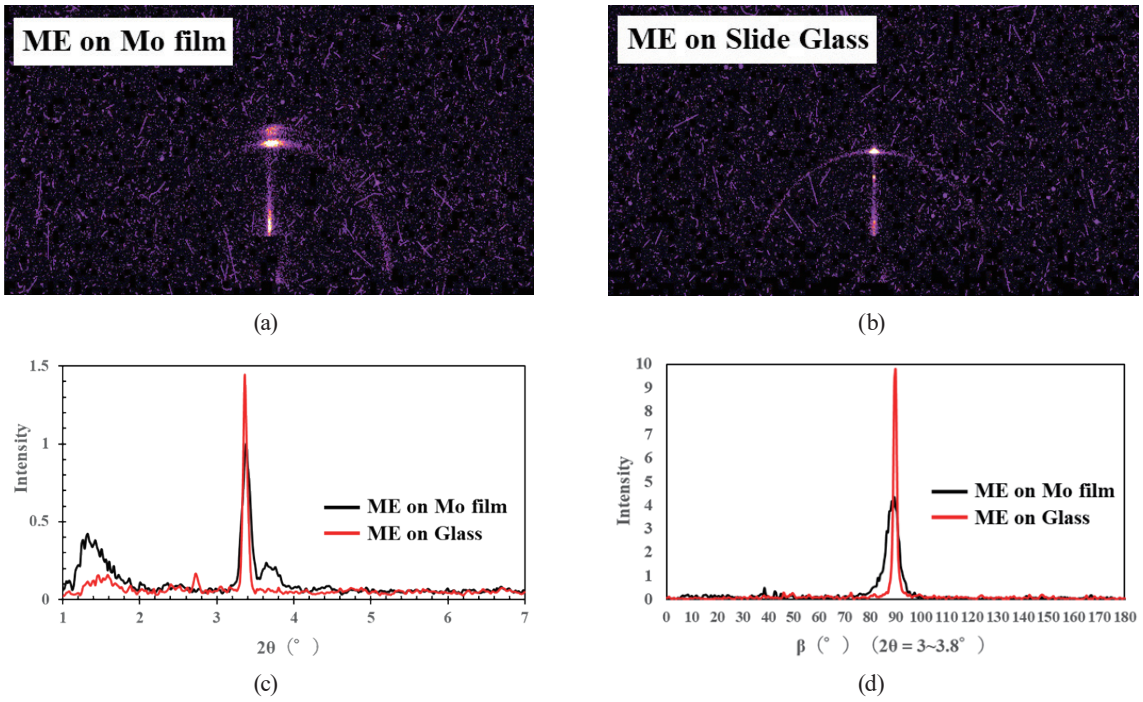

Fig. 4. (Color online) (a), (b) 2D images at a camera length of 300 mm, (c) 2θ profile, and (d) β scan profile.

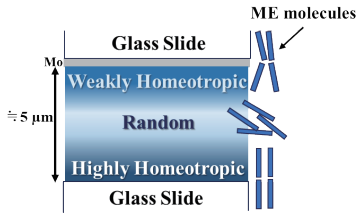

Fig. 5. (Color online) Molecular orientation image of ME, estimated from XRD measurement results.

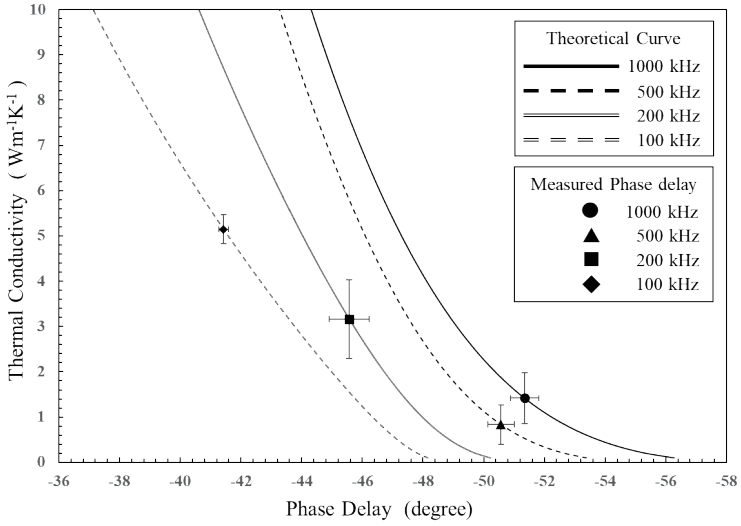

Fig. 6. Theoretical curves of phase delay vs thermal conductivity at each heating frequency, along with the phase delay obtained through measurements.

conductivity is obtained through inverse analysis by matching the theoretical curve to the measured phase delay, a small variation in phase delay directly produces a corresponding shift in fitted thermal conductivity. Therefore, the vertical error bars were evaluated by repeating the inverse analysis within the experimentally observed range of phase-delay variation. Table 2 shows the thermal conductivity values estimated from Fig. 6, along with the thermal diffusion lengths calculated from Eq. (1), using the thermal conductivity, density, and specific heat capacity.

As shown in Table 2, decreasing the modulation frequency and increasing the thermal diffusion length result in a clear increase in effective thermal conductivity. The thermal diffusion length (0.5–3.2 μm) was calculated from the estimated thermal conductivity and compared with the ME film thickness of ~5 μm. At higher frequencies, the diffusion length was much smaller than the film thickness, whereas at lower frequencies, it became comparable to that of the entire film, indicating that the measured response progressively reflected the heat transport across a larger depth region. At 1 MHz, the effective thermal conductivity was estimated to be approximately 1.41 $W \cdot m^{-1} \cdot K^{-1}$, whereas at 200 and 100 kHz, the values increased to approximately 3.16 and 5.15 $W \cdot m^{-1} \cdot K^{-1}$, respectively. In contrast, the measurement at 500 kHz yielded a lower value of 0.83 $W \cdot m^{-1} \cdot K^{-1}$, deviating from the monotonic trend observed at other frequencies. This behavior could be interpreted in terms of the molecular orientation model presented in Fig. 5. At 1 MHz, the short thermal diffusion length implied that the measurement was mainly sensitive to the Mo/ME interface region, which exhibited vertical alignment but relatively weak ordering, leading to a low effective conductivity. At 500 kHz, the thermal diffusion length increased to include not only the Mo interface but also the central region with random orientation; therefore, the effective conductivity appeared to be lower when averaged over these contributions. Although the Mo-side region was described as "weakly ordered," it still contained a notable vertically aligned component and thus exhibited a higher intrinsic thermal conductivity than the random region. In contrast, the randomly oriented region exhibited the strongest loss of orientational order, resulting in enhanced phonon scattering and the lowest intrinsic conductivity within the film. Consequently, the average conductivity across the combined region (random + weakly ordered) was lower than that of the weakly ordered region alone, leading to a relatively small value being observed at 500 kHz. At frequencies of 200 kHz and below, the diffusion length became sufficiently large, enabling contributions from the highly ordered vertically aligned region near the glass interface, resulting in a significant increase in effective conductivity. Although the thermal diffusion length at 200 kHz (~1.79 μm) reached the depth of the highly ordered region, its contribution was considered limited because the thermal

Table 2
Estimated thermal conductivity and calculated thermal diffusion length of ME for various measurement frequencies.

Modulation frequency (kHz)	Thermal conductivity ($Wm^{-1}K^{-1}$)	Thermal diffusion length (μm)
1000	1.41	0.54
500	0.83	0.58
200	3.16	1.79
100	5.15	3.23

sensitivity decreased exponentially with depth and the ordered region was relatively thin. Even so, its intrinsically higher thermal conductivity meant that a small overlap was sufficient to slightly increase the effective conductivity, compared with that at 500 kHz. Thus, the frequency-dependent variation in thermal conductivity observed in this study was consistent with the assumed molecular orientation–distribution model of ME thin films.

Furthermore, the thermal conductivity values obtained in this study were substantially higher than those of conventional epoxy resins (0.17–0.21 $W \cdot m^{-1} \cdot K^{-1}$),[1] indicating that ME inherently exhibited a high thermal transport capability. The values observed at low frequencies (3–5 $W \cdot m^{-1} \cdot K^{-1}$) were also comparable to the previously reported conductivities of vertically aligned ME resins,[10,11] demonstrating consistency with the results of earlier studies. The present measurement approach using a glass slide is applicable to materials for which the direct sputter deposition of Mo thin films is not feasible, such as polymers, adhesives, and flexible samples that are difficult to separate. Therefore, this method is expected to be useful for evaluating the thermal conductivities of a wide range of materials.

4. Conclusions

In this study, the thermal conductivities of ME thin films were evaluated using the periodic heating thermoreflectance method, based on an analytical model in which a semi-infinite glass substrate was introduced as the zeroth layer. This approach utilized an existing three-layer analytical model and replaced the semi-infinite air layer with a semi-infinite glass layer to better represent the actual experimental configuration. This simple, yet effective, substitution maintained the theoretical consistency of the original model, while facilitating the realistic evaluation of the samples measured on a glass slide. Lowering the modulation frequency increased the effective thermal conductivity. This behavior could be explained by the increase in thermal diffusion length, which sequentially included contributions from the weakly ordered vertically aligned region near the Mo interface, central randomly orientated region, and highly ordered vertically aligned region near the glass interface. These findings indicated a correlation between the molecular orientation and thermal transport in ME thin films. The effective thermal conductivities obtained in this study were significantly higher than those of conventional epoxy resins (0.17–0.21 $W \cdot m^{-1} \cdot K^{-1}$). However, the values observed at low frequencies (3–5 $W \cdot m^{-1} \cdot K^{-1}$) were comparable to those previously reported for vertically aligned ME resins. Overall, the present approach, based on the simple replacement of the air layer with a glass layer in the existing three-layer analytical model, proved to be both theoretically sound and experimentally practical and can be a useful method for evaluating the thermal conductivities of materials on which direct Mo deposition is difficult, such as polymers, adhesives, and soft substrates.

Acknowledgments

The authors express their sincere gratitude to Mr. Yusuke Ohori of the Open Facility Center, Ibaraki University, for his support with the two-dimensional grazing-incidence small-angle X-ray scattering (GI-SAXS) measurements and analysis performed using the Rigaku SmartLab system.

References

1 M. Akatsuka and Y. Takezawa: J. Appl. Polym. Sci. **89** (2003) 2464. https://doi.org/10.1002/app.12489
2 K. Fukushima, H. Takahashi, Y. Takezawa, T. Kawahira, M. Itoh, and J. Kanai: IEEJ Trans. Fund. Mater. **126** (2006) 1167. https://doi.org/10.1541/ieejfms.126.1167
3 S. Song, H. Katagi, and Y. Takezawa: Polymer **53** (2012) 4489. https://doi.org/10.1016/j.polymer.2012.07.065
4 Y. Li, P. Badrinarayanan, and M. R. Kessler: Polymer **54** (2013) 3017. https://doi.org/10.1016/j.polymer.2013.03.043
5 H. Chen, V. V. Ginzburg, J. Yang, Y. Yang, W. Liu, Y. Huang, L. Du, and B. Chen: Prog. Polym. Sci. **59** (2016) 41. http://dx.doi.org/10.1016/j.progpolymsci.2016.03.001
6 R. Maeda, K. Okuhara, A. Nakamura, T. Hayakawa, Y. Uehara, T. Motoya, and H. Nobutoki: Chem. Lett. **45** (2016) 795. https://doi.org/10.1246/cl.160249
7 T. Tanase, T. Kato, S. Tanaka, A. Sano, H. Kojima, and K Fukushima: IEEE Trans. Dielectr. Electr. Insul. **25** (2018) 2212. https://doi.org/10.1109/TDEI.2018.007415
8 M. Lee, T. Tanase, T. Kato, S. Tanaka, A. Sano, H. Kojima, and K. Fukushima: Nanoscale Adv. **4** (2022) 1970. https://doi.org/10.1039/d1na00896j
9 R. Marui, H. Maeda, K. Hatakeyama-Sato, Y. Nabae, and T. Hayakawa: Macromolecules **57** (2024) 11221. https://doi.org/10.1021/acs.macromol.4c00506
10 S. Tanaka, F. Hojo, Y. Takezawa, K. Kanie, and A. Muramatsu: ACS Omega **3** (2018) 3562. https://doi.org/10.1021/acsomega.7b02088
11 S. Tanaka, Y. Takezawa, K. Kanie, and A. Muramatsu: ACS Omega **5** (2020) 20792. https://doi.org/10.1021/acsomega.0c01603
12 N. Tang, S. Tanaka, Y. Takezawa, and K. Kanie: J. Appl. Polym. Sci. **138** (2021) 7. https://doi.org/10.1002/app.51396
13 Y. Takezawa and R. Fukuta: J. Netw. Polym. Jpn. **44** (2023) 129. https://doi.org/10.11364/networkedpolymer.44.3_129
14 K. Hatori, N. Taketoshi, T. Baba, and H. Ohta: Rev. Sci. Instrum. **76** (2005) 4901. https://doi.org/10.1063/1.2130333
15 T. Yagi, N. Taketoshi, and H. Kato: Physica C **412–414** (2004) 1337. https://doi.org/10.1016/j.physc.2003.12.087
16 K. Hatori, K. Suzuki, H. Fukuyama, and H. Ohta: Heat Transf. – Asian Res. **38** (2009) 57. https://doi.org/10.1002/htj.20227
17 T. Nishi, T. Mayama, H. Ohta, and Y. Okamoto: Sens. Mater. **31** (2019) 743. https://doi.org/10.18494/SAM.2019.2119
18 S. Ito, S. Kuroe, T. Nishi, H. Ohta, T. Ikeda, and K. Hatori: Netsu Bussei **35** (2021) 49 (in Japanese). https://doi.org/10.2963/jjtp.35.49
19 R. Endo, Y. Suganuma, K. Endo, T. Nishi, H. Ohta, and S. Tachikawa: Int. J. Thermophys. **43** (2022). https://doi.org/10.1007/s10765-022-03031-y
20 N. Kudo, S. Watanabe, T. Nishi, H. Ohta, S. Tachikawa, and R. Endo: High Temp. Mater. Process. **44** (2025) 20240068. https://doi.org/10.1515/htmp-2024-0068
21 G. Matsui and H. Kato: Rev. Sci. Instrum. **82** (2011) 034905. https://doi.org/10.1063/1.3557389
22 H. Ohta, K. Hatori, G. Matsui, T. Yagi, S. Miyake, T. Okamura, R. Endo, R. Okada, K. Morishita, S. Yokoyama, K. Taguchi, and H. Kato: Meas. Sci. Technol. **27** (2016) 115002. https://doi.org/10.1088/0957-0233/27/11/115002
23 S. Miyake, G. Matsui, H. Ohta, K. Hatori, K. Taguchi, and S. Yamamoto: Meas. Sci. Technol. **28** (2017) 075006. https://doi.org/10.1088/1361-6501/aa72d0

About the Authors

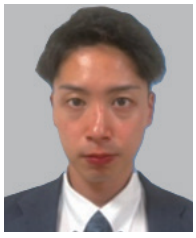

Naoto Kudo received his B.S. degree from the National Defense Academy (NDA), Japan, in 2019, and his M.S. degree from Ibaraki University, Japan, in 2024. Since 2024, he has been a Ph.D. student at Ibaraki University. His research interests include the thermoreflectance method, thermal microscope, polymer materials, and thin-film materials. (24nd152g@vc.ibaraki.ac.jp)

Yoshitaka Takezawa received his B.E., M.E., and Ph.D. degrees in Applied Chemistry from the Keio University, Japan, in 1985, 1987, and 1993, respectively. He joined Hitachi Ltd., Japan, in 1987. Since 2008, he has been working for Hitachi Chemical Co., Ltd. (currently known as Resonac Corporation), where he has been focusing on insulating polymer materials, especially high-thermal-conductivity mesogenic resins. Since 2021, he has also been a visiting professor (concurrent position) at Ibaraki University.
(takezawa.yoshitaka.xigpt@resonac.com)
(yoshitaka.takezawa.pq15@vc.ibaraki.ac.jp)

Tsuyoshi Nishi received his B.S. degree from the Tokyo University of Science, Japan, in 1999, and his M.S. and Ph.D. degrees from Tohoku University, Japan, in 2001 and 2004, respectively. From 2004 to 2021, he served as a Research Scientist at the Japan Atomic Energy Agency and an associate professor at Ibaraki University, Japan. Since 2021, he has been a professor at Ibaraki University. His research interests include thermophysical properties, structural analysis, noncrystalline materials, and nuclear materials.
(tsuyoshi.nishi.75@vc.ibaraki.ac.jp)

Hiromichi Ohta received his B.S., M.S., and PhD degrees from Tohoku University, Japan, in 1978, 1980, and 1984, respectively. From 1984 to 2008, he was a research associate and an associate professor at Ibaraki University, Japan. Since 2008, he has been a professor at Ibaraki University. His research interests include thermophysical properties, computational materials science, composite materials, and silicate melts. (hiromichi.ohta.ys@vc.ibaraki.ac.jp)